J. theor. Biol. (2000) **205,** 201–214
doi:10.1006/jtbi.2000.2061, available online at http://www.idealibrary.com on IDEAL®

Lessons on Pattern Formation from Planet WATOR

RICK DURRETT*† AND SIMON LEVIN‡

** Department of Mathematics, Cornell University, Ithaca, NY 14853, U.S.A. and*
‡ Ecology and Evolutionary Biology, Princeton University, Princeton, NJ 08544, U.S.A.

(*Received on* 30 *July* 1999; *Accepted in revised form on* 22 *March* 2000)

It is well known that if reacting species experience unequal diffusion rates, then dynamics that lead to a constant steady state in a "well-mixed" environment can in a spatial setting lead to interesting patterns. In this paper, we focus on complementary pattern formation mechanisms that operate even when the diffusion rates are equal. In particular, we can say that when the mean-field ODE has an attracting periodic orbit then the stochastic spatial model will have large-scale spatial structures in equilibrium. We explore this mechanism in depth through the dynamics of the simulator WATOR.

1. Introduction

Predator-prey systems in nature show a variety of spatial and spatio-temporal patterns. In part, these are attributable to underlying physical features of the environment, such as soil factors or turbulent flow patterns (Levin, 1992); in part, they are self-organized, emerging from the rules of individual behavior (Flierl *et al*., 1999). Whatever the causes, such patterns are of fundamental ecological and evolutionary consequence, holding the key to understanding the maintenance of biological diversity.

The usual mathematical approach to exploring spatial patterns is through the use of reaction–diffusion equations. These equations can support a wide range of solutions, from spatially uniform patterns, to non-uniform stationary ones, to plane waves and spiral waves. In all of these, the local interaction rules control the range of possible global behaviors, though unequal diffusion rates can complicate the picture.

One of the fundamental issues in any branch of science is how processes on small scales can produce patterns on much larger scales. In a seminal paper, Turing (1952) showed that, in reaction– diffusion equations, spatial patterns can arise from a combination of chemical reaction and diffusion provided the diffusion rates differ sufficiently. Turing's paper is at the core of many theories of the development of biological pattern and form, see Murray (1989, 1990).

Following Turing's example, a reaction-diffusion system is said to exhibit *diffusion-driven instability* if the homogeneous steady state is stable to small perturbations in the absence of diffusion, but unstable to small spatial perturbations when diffusion is present. In Turing's case, the appearance of patterns is due to a combination of short-range activation and long-range inhibition. Segel & Jackson (1972) were the first to show how the effects of random dispersal in predator–prey models could lead to similar diffusive instabilities.

These ideas were developed further by Levin (1974), Levin & Segel (1976) and Segel & Levin (1976), who studied systems with an autocatalytic or "Allee effect," meaning that, for some range of

†Author to whom correspondence should be addressed.

0022–5193/140201 + 14 $35.00/0

densities, the per capita rate of growth is an increasing function. This could be due, for example, to an increased efficiency of predation when densities of prey increase. Stable patterns can arise through diffusive instability when there is an Allee effect in the prey density (Segel & Jackson, 1972; Levin, 1974), or in the predator density if the prey diffusion rate is sufficiently high (Levin, 1974).

In the other direction, Mimura (1979) and Mimura *et al.* (1979) showed that if the density of prey N and predator P satisfy

$$N_t = d_1 N_{xx} + N(h(N) - P),$$

$$P_t = d_2 P_{xx} + P(N - k(P)),$$

where $h(N)$ is decreasing in N and $k(P)$ is increasing in P then the solution tends to be spatially homogeneous asymptotically. Comparing with the work of Levin and Segel, we can say that an Allee effect is necessary for patchiness to result from a diffusion-driven instability in this system. For a survey on pattern formation by this mechanism, see Levin & Segel (1985).

A second recipe for spatial structure to arise in exploiter–victim systems can be found in the work of Hassell *et al.* (1991). They considered mathematical models for host–parasitoid interactions, where in each patch the densities of host and parasitoid follow the difference equations of the Nicholson–Bailey model

$$N_{t+1} = \lambda N_t e^{-aP_t},$$

$$P_{t+1} = qN_t(1 - e^{-aP_t})$$

and in each generation specified fractions (μ_N and μ_P) of the host and parasitoid populations migrate to adjacent patches. They found that these models exhibited a remarkable range of behaviors, from spiral waves and spatially chaotic variation to static "crystal lattice" patterns.

Nowak & May (1992, 1993), Nowak *et al.* (1994) and May (1994, 1995) followed up on this important work by considering the classical Prisoner's dilemma game in a spatial setting. They found that the simple introduction of a spatial dimension to the competition, with no memories among the players and no elaboration of the available strategies, could generate chaotically changing spatial patterns in which cooperators (victims) and defectors (exploiters) both persist indefinitely in the population. For a stochastic spatial approach to these "evolutionary games", see Durrett & Levin (1994).

The host–parasitoid and Prisoner's dilemma examples just discussed are remarkable because in each case a self-organized spatial heterogeneity stabilizes an interaction that is unstable in a single homogeneously mixing population. In this paper, we will extend these considerations to situations in which a homogeneously mixing system has an attracting periodic orbit. It has long been known that in this situation the corresponding reaction–diffusion equation will have interesting spatial structures. Kopell and Howard showed that if the ordinary differential equation (ODE) for the homogeneously mixing system has a stable periodic orbit then the corresponding reaction diffusion equation will have plane wave solutions (Kopell & Howard, 1973) and spiral wave solutions (Kopell & Howard, 1981).

As Kopell & Howard (1974) explained, they were motivated by the observation of spiral waves in the Belousov–Zhabotinsky reaction. For more details about this fascinating system, see the book by Winfree (1987) or Sections 10.1 and 12.3 in Murray's (1989) book. Here we have a different inspiration: the study of predator–prey systems. Furthermore, we will pursue our study in the context of stochastic spatial models rather than reaction-diffusion equations, since such systems more realistically represent the interaction between discrete individuals (Durrett & Levin, 1994).

The first experimental spatial system for studying predator–prey dynamics was created by Huffaker (1958) who used rectangular arrays of partially peeled oranges and rubber balls to study the interactions between two species of mites. He and many others who later performed similar experiments found that while small systems were highly unstable and broke down after one or two population cycles, larger systems were considerably more robust. Pimentel *et al.* (1963) complemented Huffaker's classic work, again demonstrating experimentally how self-organized spatial heterogeneity can lead to the

persistence of unstable predator–prey interactions.

Hilborn (1975) provided the first real theoretical examination of Huffaker's experimental system, creating a computer model to mimic it. Hilborn's model is what we would now call a metapopulation model. See Hanski & Gilpin (1996) and Hanski (1998). The environment was made up of patches linked through movement, with every patch having equal access to every other. Within each patch, population density was modeled according to a system of difference equations. Hilborn found a range of behaviors, from system collapse to long-range persistence, depending on parameter values. Increasing the size of the system increased persistence, as anticipated by Maynard Smith (1974).

Nachman (1987a, b) seems to have been the first to simulate Huffaker's system as a truly spatial model. Since that time a number of papers have investigated the impact of the spatial distribution of competitors on the behavior of predator–prey systems (see DeRoos *et al*., 1991; McCauley *et al*., 1993; Wilson *et al*., 1993; Satulovsky & Tome, 1994; Rand *et al*., 1995; Neubert *et al*., 1995; Wilson, 1996; Comins & Hassell, 1996; Satulovsky, 1996; Pascual & Caswell, 1997).

In our previous work, we have shown that the outcome of spatially explicit interactions depends fundamentally on the way a system is modeled. The metapopulation approach of Hilborn (1975); see also Chesson (1981, 1985), can capture many of the features of the spatial localization of interactions, but can also produce results that differ qualitatively from explicit spatial formulations, such as reaction–diffusion equations. A concrete example of this occurs in the Prisoner's Dilemma case of Durrett & Levin (1994). The problem in that example, and in real populations, is that individuals are not infinitesimals. Thus, when two interacting species reach densities that are low enough, they lose contact with each other and cease to interact, in contrast to the situation represented by the reaction–diffusion equation. The problem is more severe for spatially distributed systems than well-mixed ones, because population densities must inexorably reach low levels at many points in a habitat.

In this paper, we complement previous work by examining an individual-based stochastic spatial model. The system we study is a simplification of a discrete time (probabilistic) cellular automaton called WATOR, short for WAter TORus. This model was developed by David Wiseman at the University of Western Ontario and was discussed in A.K. Dewdney's *Computer Recreations* column in *Scientific American* in December 1984. It has the novel feature that the predator's level of hunting is controlled by a parameter q, and increasing q beyond 3 can lead to a limit cycle in the corresponding ODE via Hopf bifurcation.

Our aim in this investigation is not only to analyse this interesting phenomenon but also to continue to develop a program begun in Durrett & Levin (1994) of classifying the behavior of stochastic spatial models. There it was proposed that the behavior of stochastic spatial models could be determined from the properties of the mean-field ODE that is obtained by pretending that the states of all sites are always independent. WATOR fits into Case 3, which is defined (see Durrett, 1999) as "periodic orbits in the mean-field ODE", so their scheme predicts: "in the spatial model, densities oscillate like the ODE on small length scales, but on large length scales are almost constant (after an initial transient). That is, there is an equilibrium state with an interesting spatial structure".

In Section 2, we introduce Dewdney's original discrete time WATOR model, then strip away irrelevant complications to formulate the simplified continuous time version we will study. In Section 3, we derive the mean-field ODE that results by pretending that adjacent sites are always independent, find the only interesting fixed point, and then investigate the stability of this fixed point to show the existence of a Hopf bifurcation producing a periodic orbit.

In Section 4, we introduce the reaction–diffusion equation that occurs as the fast stirring limit of the stochastic spatial model and use this connection to prove that on an infinite lattice our stochastic spatial model has a stationary distribution in which predator and prey coexist. In Section 5, we will use simulations to investigate the structure of this equilibrium state. Note that in contrast to Turing's results, spatial patterning

occurrs here in a system with equal diffusion rates.

2. The WATOR Model

We begin by describing the original WATOR model in detail to make the point that models are often easier to formulate in continuous time. Time is discrete ($t = 0, 1, \ldots$) with the action taking place on the square lattice, the points in the plane with integer coordinates. Each site can be in one of three states: 0 = vacant, 1 = prey (fish), and 2 = predators (sharks). Furthermore, each shark and each fish has an *age*, and each shark has a *hunger index*, which indicates the number of days since it has eaten.

The array is updated by sequentially applying four procedures called FISHMOVE, FISHBIRTH, SHARKMOVE, and SHARKBIRTH to the entire grid. To be able to describe these, we declare the *neighbors* of a site x to be the eight sites y adjacent or diagonally adjacent to x:

$$\begin{matrix} y & y & y \\ y & x & y \\ y & y & y. \end{matrix}$$

Later, we will use other choices of neighborhood; therefore, note that the rules below do not depend on the exact definition of neighbor.

FISHMOVE: For each site that is occupied by a fish, the program makes a list of unoccupied neighbors and moves the fish to one of these chosen at random. The fish gets one day older.

FISHBIRTH: If the fish's age is *fbreed*, the program puts a new fish at the old position and gives age 0 to both mother and daughter. From the ages, one can see that we are thinking of these fish as two children rather than mother and daughter.

SHARKMOVE: A shark first chooses randomly without replacement q of its neighboring sites. There are two cases to consider:

(a) If the shark finds no fish, it moves to a randomly chosen neighboring site that is unoccupied. The *hunger index* for that shark is increased by one. If the hunger index now exceeds the cutoff *starve*, the shark dies. Otherwise, it gets one day older.

(b) If the shark finds one or more fish, it picks one at random, moves there and eats it. The *hunger index* is set equal to 0, but it does age one day.

SHARKBIRTH: If the shark's age is *sbreed*, the program puts a new shark at the old position and gives age 0 and hunger index 0 to both.

The description above is taken (with some minor editing) from page 20 of Dewdney's column. As in many discrete time systems, there is the question of what to do when *collisions occurs*, e.g. when two fish choose to move to the same vacant site, or when two sharks try to eat the same fish. For this reason, and because the density of sharks or fish can change considerably (e.g. by 10 or 20%) in one of these steps, we will reformulate the model in continuous time.

A second simplification that we will make is to eliminate the age variables and replace them by coin flips, i.e. rather than a fish giving birth after a fixed number of days, it will breed (on the average) once every *fbreed* days. In discrete time this can be done by flipping a coin at each time and for each site with a probability 1/*fbreed* of getting heads. In continuous time, each site will try to breed at times of a Poisson process with rate 1/*fbreed*, in which the times between occurrences are exponentially distributed with mean *fbreed* days. Treating the events that affect the sharks in a similar way, we arrive at the following model. Again the reader can see that the description makes sense for any definition of neighbors.

(i) Fish are born at vacant sites at rate β_1 times the fraction of neighbors occupied by fish.

(ii) At rate 1 each shark inspects q neighboring sites, chosen without replacement from the neighbor set. It moves to the first fish it finds and eats it. A shark that has just eaten gives birth to a new shark left on its starting square with probability β_2. A shark that finds no fish does not move and dies with probability δ.

(iii) There is *stirring* (also called *swimming*) at rate v: for each pair of nearest-neighbor sites x and y we exchange the values at x and at y, at rate v.

The stirring mechanism automatically preserves the restriction of at most one individual per site and has the mathematical advantage that the trajectory of any single particle is just a continuous time random walk. Of course, if one watches the movements of two particles there is a (very small) correlation between their locations due to the occasional stirring steps that affect both particles at the same time.

3. Mean-field Theory

Stirring breaks down the correlations between neighbors that develop from the birth and death steps in the predator–prey interaction. When the rate of stirring is much larger than the total of all the birth and death rates, we expect that adjacent sites will always be almost independent. This fact can be proved rigorously and will be the basis of our analysis in the next section. However, for the moment, we simply view this claim as motivation for writing down the *mean-field ODE* that is obtained by letting $u_i(t)$ be the fraction of sites in state i at time t, and computing the rate of change by supposing that all sites are always independent:

$$\begin{aligned} du_1/dt &= \beta_1 u_1(1-u_1-u_2) - u_2\{1-(1-u_1)^q\}, \\ du_2/dt &= \beta_2 u_2\{1-(1-u_1)^q\} - \delta u_2(1-u_1)^q. \end{aligned} \tag{1}$$

Here, the first term on the right represents the birth of fish onto vacant sites. To explain the second and third terms, we note that $u_2\{1-(1-u_1)^q\}$ gives the fraction of sites occupied by sharks times the probability a given shark will find at least one fish when it inspects q neighbors, so multiplying by the probability of birth β_2 gives the rate at which new sharks are produced. For similar reasons, the fourth term represents the sharks who find no fish to eat, and died with probability δ.

To begin to understand the ODE we note that in the absence of fish, sharks can not breed and their density drops to 0. Conversely, in the absence of sharks, fish do not die and will fill up the space. The last two results give the direction of motion of the ODE on two sides of the right triangle that we use for the possible states of the system: $\Gamma = \{(u_1, u_2)\colon u_1, u_2 \geqslant 0,\ u_1 + u_2 \leqslant 1\}$.

Since fish do not die in the absence of sharks, there is a boundary equilibrium at (1, 0). Considering the second equation in eqn (1) and setting $u_1 = 1 - \varepsilon_1$ and $u_2 = \varepsilon_2$ where the ε_i are small shows that (1, 0) is always a saddle point. This behavior suggests the presence of a fixed point $(\bar{u}_1, \bar{u}_2)$ with both components positive, a fact which can easily be confirmed by algebraic manipulation. To do this neatly, and to pave the way for later calculations, we will first rewrite the system in eqn (1) as

$$\begin{aligned} du_1/dt &= A(u_1) - u_2 B(u_1), \\ du_2/dt &= u_2 C(u_1), \end{aligned} \tag{2}$$

where $A(u_1) = \beta_1 u_1(1-u_1)$,

$$B(u_1) = \beta_1 u_1 + \{1-(1-u_1)^q\}$$

and $C(u_1) = \beta_2 - (\beta_2 + \delta)(1-u_1)^q$. In order for $du_2/dt = 0$ we must have

$$C(\bar{u}_1) = 0 \quad \text{or} \quad \bar{u}_1 = 1 - \left(\frac{\beta_2}{\beta_2 + \delta}\right)^{1/q}. \tag{3}$$

Having found $\bar{u}_1$ we can now set $du_1/dt = 0$ to find

$$\bar{u}_2 = A(\bar{u}_1)/B(\bar{u}_1). \tag{4}$$

To investigate the nature of the fixed point at $(\bar{u}_1, \bar{u}_2)$, we let $v_i = u_i - \bar{u}_i$ be the displacement in the i-th component. Assuming the v_i are small and using eqns (3) and (4), we arrive at the linearized equation

$$\begin{aligned} dv_1/dt &= Fv_1 + Gv_2, \\ dv_2/dt &= Hv_1, \end{aligned}$$

where $F = A'(\bar{u}_1) - \bar{u}_2 B'(\bar{u}_1)$, $G = -B(\bar{u}_1)$, and $H = u_2 C'(\bar{u}_1)$. This ODE is analysed in Appendix A with the following result.

Theorem 1. *The interior fixed point is always locally attracting when $q \leqslant 3$. Conversely, if $q > 3$ and the values of β_2 and δ are held constant,*

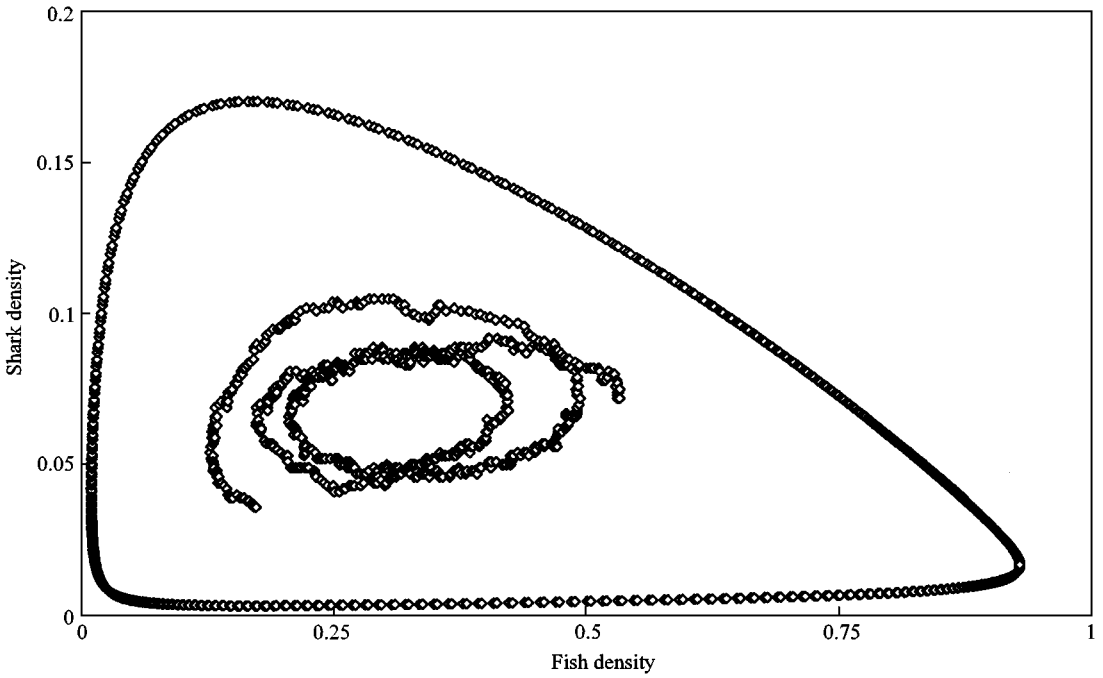

FIG. 1. An example of the WATOR ODE with a limit cycle, (the smooth outside curve). The irregular curve gives the observed frequencies in a 64×64 viewing window.

decreasing β_1 leads to a Hopf bifurcation that produces a limit cycle.

Figure 1 gives a picture of a case of the ODE with a limit cycle: $q = 8$ with $\beta_1 = 1/3, \beta_2 = 1/10$, and $\delta = 1/3$. The limit cycle is the smooth outer curve.

4. Reaction Diffusion Equations and WATOR

To make connections between our model and reaction–diffusion equations, we will suppose that the stirring rate v is large and consider our process on a scaled version of the square lattice in which the spacing between sites is reduced to $v^{-1/2}$. De Masi *et al.* (1986) have shown (see also Durrett & Neuhauser, 1994, or Section 8 of Durrett, 1995) that as v tends to infinity, the densities of fish and sharks converge to the solution of the partial differential equation:

$$\begin{aligned} \partial u_1/\partial t &= \Delta u_1 + g_1(u_1, u_2) \\ \partial u_2/\partial t &= \Delta u_2 + g_2(u_1, u_2) \end{aligned} \tag{5}$$

where the g_i are the right-hand sides of the mean-field ODE in eqn (1). Our next result, proved in Appendix A, says that sharks and fish coexist in the reaction-diffusion equation.

Theorem 2. *Suppose that the initial conditions $u_i(x, 0)$ are continuous, always in the set Γ of sensible values, and have $u_i(0, x) \geqslant \eta_i > 0$ on $[-\delta, \delta]^2$. There are constants $\kappa, \varepsilon_i > 0$ and $t_0 < \infty$, which only depend on η_i and δ so that $u_i(x, t) \geqslant \varepsilon_i$ whenever $|x| \leqslant \kappa t$ and $t \geqslant t_0$.*

Here $|x| = (x_1^2 + x_2^2)^{1/2}$ is the usual Euclidean distance.

Theorem 2 says that the densities of all types stay bounded away from zero on a linearly growing set. In words, both species persist in the reaction–diffusion equation. Using methods of Durrett & Neuhauser (1994), we can convert Theorem 2 into a similar conclusion about the particle system. Recall that π is a said to be a *stationary distribution* if when the initial state ξ_0 has this distribution then so does the state at time t, ξ_t, for all $t > 0$. In words, a stationary distribution represents an equilibrium state for the process.

Theorem 3. *When the stirring rate is large there is coexistence, i.e. there is a stationary distribution for the particle system that concentrates on configurations with infinitely many sites in each of the possible states.*

Proof. Theorem 2 implies that the assumptions of Theorem 9.1 of Durrett (1995) are satisfied and the desired conclusion follows. □

5. Simulations of the Particle System

The result in Theorem 3 proves the existence of a stationary distribution but gives no insight into its properties. We would like to understand the structure of a "typical realization" of the stationary distribution, whose existence is asserted in Theorem 3. Since the information is out of the reach of theory today, we turn to the computer. We simulated the process on a 700×700 grid with periodic boundary conditions. That is, sites along the left edge of the grid are adjacent to those on the right and those on the top edge are adjacent to those on the bottom.

Figures 2–5 show the densities of predator and prey when viewed in observation windows of size 20×20, 64×64, 125×125 and 700×700 (i.e. the whole system). As will be explained later, the choice of window sizes is governed by the correlation length. Here we chose $q = 8$ with $\beta_1 = 1/3$, $\beta_2 = 1/10$, and $\delta = 1/3$ so that we can compare with results of Pascual & Levin (1999). As predicted by Case 3 of Durrett & Levin (1994), the oscillations in the smallest window are pronounced and are reduced as the size of the window increases. However, as Fig. 1 shows, the oscillations of the densities in the 64×64 box are considerably smaller than those in the periodic orbit for the mean-field ODE. At 125×125 the oscillations are much like those at 64×64 though they are smoother and the magnitudes of the peaks are reduced. At 700×700, the curves are very smooth and show an exponentially damped oscillation as the system converges towards it stationary state. Since 700 is a finite number the oscillations will not completely go away but reach a small level as seenat time 800–1000.

In small observation windows, all the sites experience times of high density and low density

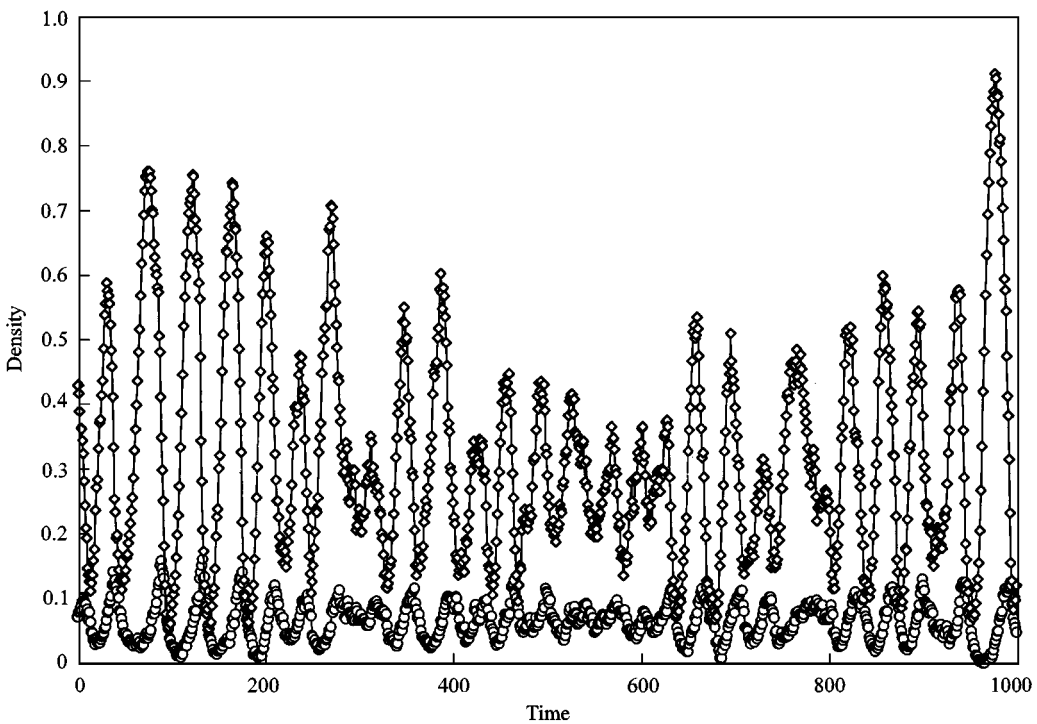

FIG. 2. The frequency of sharks (○) and fish, (◇) in a 20×20 viewing window inside a 700×700 grid.

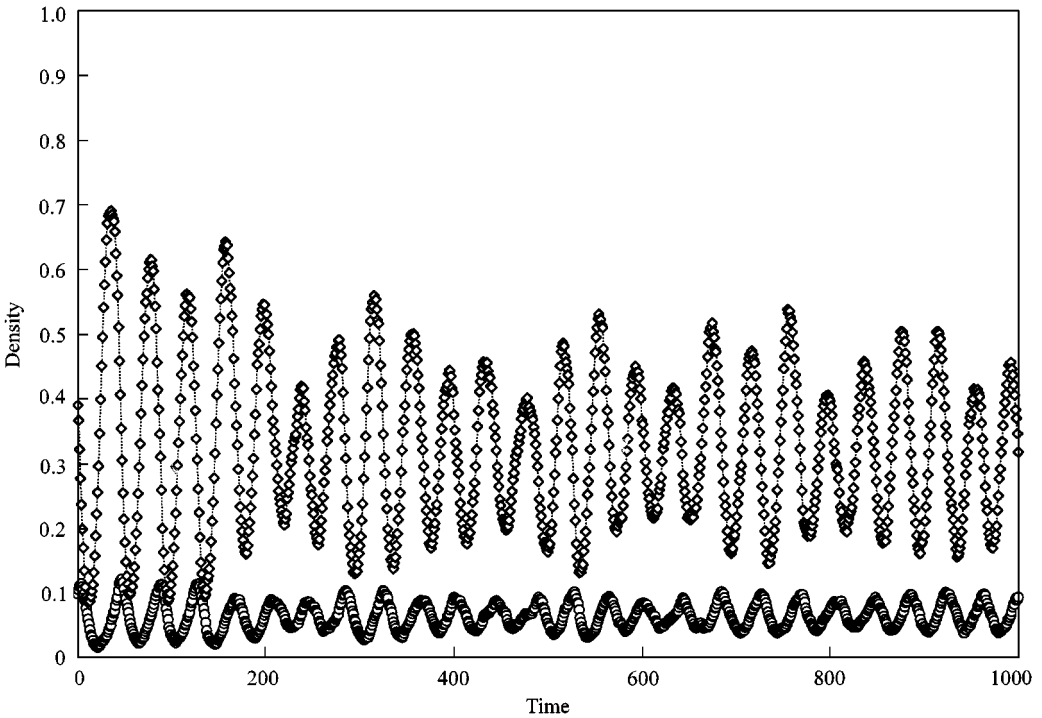

FIG. 3. The frequency of sharks (○) and fish, (◇) in a 64×64 viewing window inside a 700×700 grid.

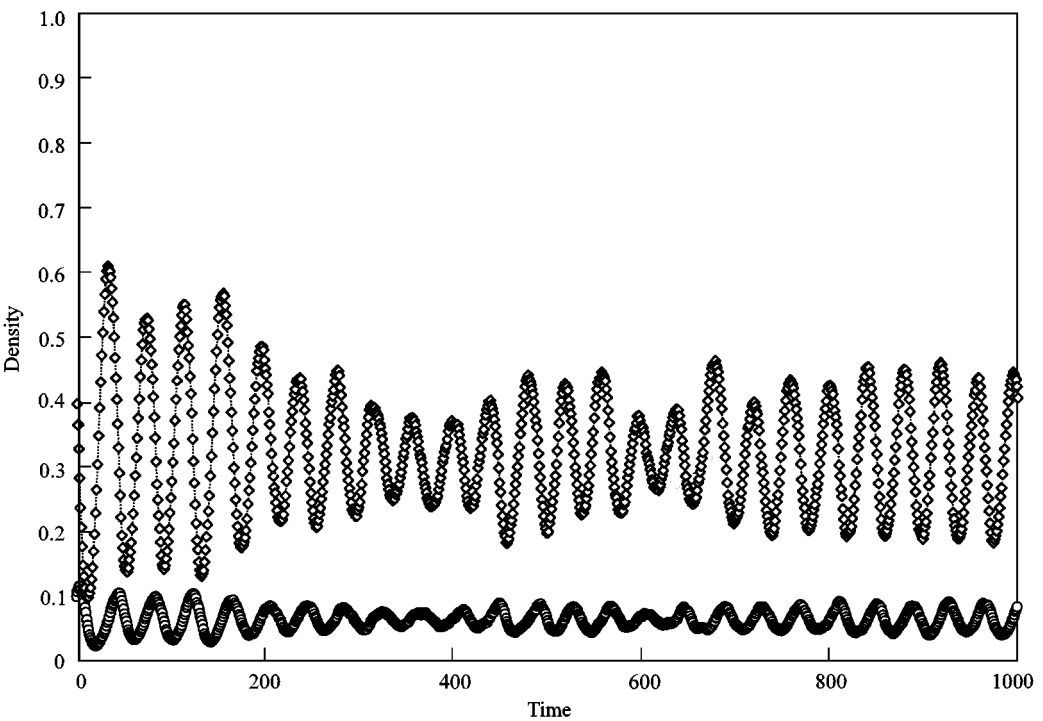

FIG. 4. The frequency of sharks (○) and fish, (◇) in a 125×125 viewing window inside a 700×700 grid.

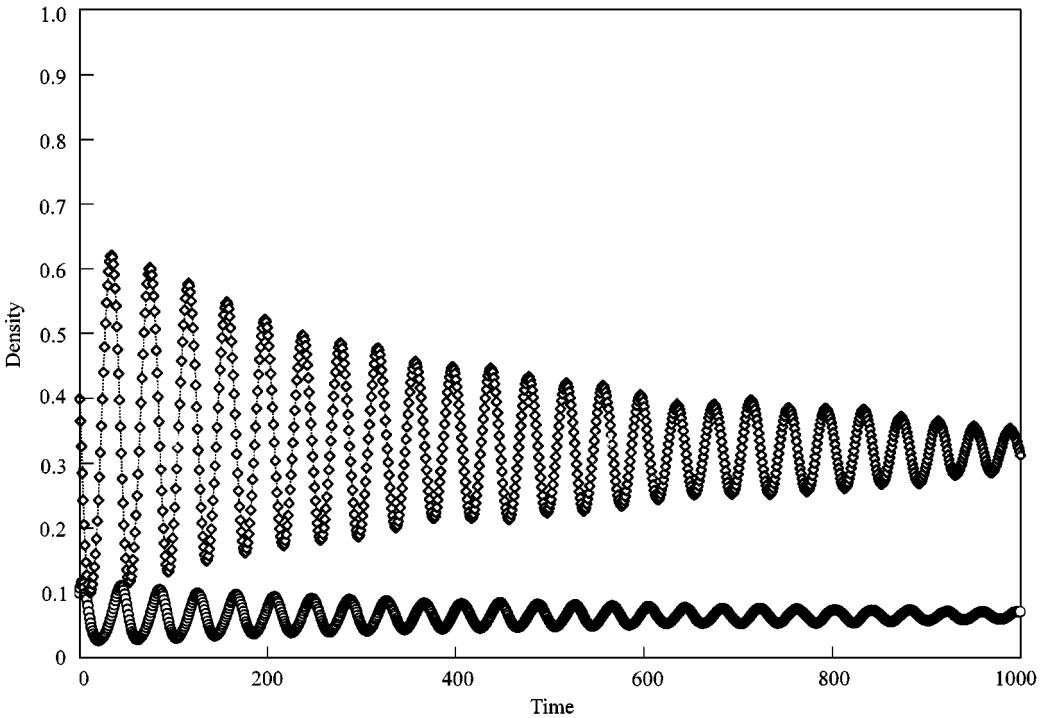

FIG. 5. The frequency of sharks (○) and fish (◇) in a 700×700 grid.

almost simultaneously, while in large windows fluctuations in different parts are out of phase and one sees something closer to the average. The length scale that represents the dividing line between small and large is called the *correlation length*. This can be defined in a number of ways. Pascual & Levin (1999) examine the time series of the densities of fish in boxes of various sizes and use ideas from dynamical systems to search for what they call the "intermediate scale of nontrivial determinism". We refer the reader to their paper for the details of its definition. For the parameters indicated above, their correlation length is 64, i.e. the size considered in Figs 3 and 1.

Rand & Wilson (1995) and Keeling *et al.* (1997) have taken a simpler approach; more closely related to that used in statistical mechanics. Let S_L be the number of fish in the $L \times L$ box $\Lambda = [1, L]^2$ in equilibrium. Letting $\mathrm{var}(S_L)$ be the variance of S_L; they look at $v(L) = \mathrm{var}(S_L)/L^2$ and define (see Keeling *et al.*, 1997, p. 1591) the *coherence length* ℓ_c to be "the point where $v(L)$ asymptotes to a constant value". For the parameter values under consideration, Pascual & Levin (1999) have computed that $\ell_c = 125$, i.e. the size box in Fig. 4.

The definition of ℓ_c in the previous paragraph has an obvious problem: defining the value as the point where the asymptotic value is reached is highly unstable. In a number of examples, it is known that all correlations are positive (see e.g. Harris, 1977), so $v(L)$ increases to its limit. In this case, as the amount of data gets large, the estimate of $\ell_c \to \infty$. This problem is easy to fix; however, we can redefine ℓ_c to be the point where $v(L)$ first exceeds 90% (or some other fixed fraction) of its asymptotic value.

There is a second improvement in the definition we would like to propose. To explain this, we let $\xi(x)$ be the number of fish at x (which will be 1 or 0), and let $\rho(z) = (\xi(x), \xi(x+z))$. Elementary formulas from statistics imply

$$\mathrm{var}(S_L) = \sum_{x,y \in \Lambda} \rho(y-x)$$

$$= \sum_{(z_1,z_2) \in (-L,L)^2} \rho(z)(L-|z_1|)(L-|z_2|). \quad (6)$$

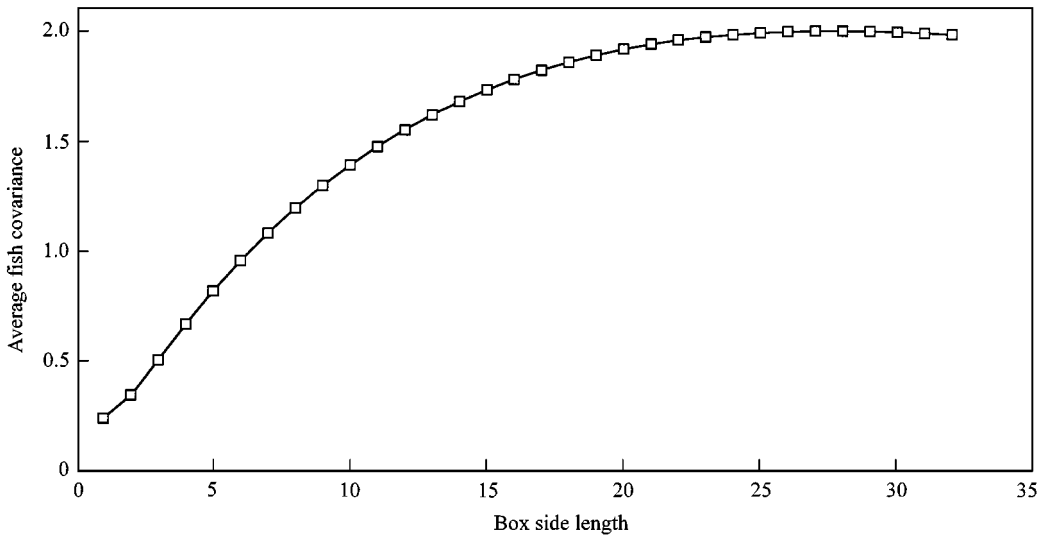

FIG. 6. Average covariance between sites inside a box of size L.

From this it follows easily that as $L \to \infty$

$$\frac{\text{var}(S_L)}{L^2} \to \sum_{z \in \mathbf{Z}^2} \rho(z). \tag{7}$$

The last result and the fact that the variance of S_L is a weighted average of the $\rho(z)$ suggests that letting ζ_c be the point where

$$\sum_{z \in [-L, L]^2} \rho(z) \tag{8}$$

first exceeds some fixed fraction of its limiting value, say 75% gives a simpler and clearer way of defining the correlation length. For a concrete example see Fig. 6. The asymptotic value for the average covariance over a box of side L is about 2. Keeling *et al.* (1997) would say that this limit is reached when $L \approx 20$ or 25. In contrast, we would compute that the average crossed 3/4's of its limiting value, i.e. 1.5, at length 11.

To close our discussion of the correlation length, we should emphasize that we are proposing a definition that is simpler and more stable, not trying to argue that our new formula gives the "right answer". Indeed, statistical mechanics tells us that the role of the correlation length is to indicate the order of magnitude of the place where correlation lengths start to decay exponentially. Like the distinction between feet and meters, the exact units in which this is measured is not important. To see that there is an important difference between the definitions of ζ_c and ℓ_c, note that if $\rho(z) = (1 - \theta)^{|z|}$ then $\zeta_c \approx K/\theta$ while $\ell_c \approx M/\theta$, where K is a constant dictated by our choice of 90% as a cutoff, and M is a value dictated by reaching the asymptotic limit. Both are multiples of $1/\theta$, however, as one has more data and hence a more estimate of the limiting curve M will continue to get larger.

6. Conclusions

When the mean-field dynamics involving two interacting species exhibit stable oscillations, corresponding interacting particle system models may sustain heterogeneous patterns even in the presence of equal movement rates. We demonstrate this by considering the predator–prey system WATOR. Proceeding first to a reaction–diffusion approximation, we conclude from existing theory that a non-trivial stationary distribution exists for the particle system. We then turn to simulations to show how characteristics of that distribution vary with window size, relating these to several different definitions of the correlation length.

Work on this project began in 1991. Semyon Kruglyak, then an undergraduate at Cornell, but now a postdoc at the University of Southern California, did

some of the first simulations in the Fall of 1992. Later that work was taken over by Linda Buttel who performed the simulations shown. Buttel has been partially supported by the Cornell Theory Center, and by NSF grant BIR-9423339 from the computational biology program. During this period Durrett has been supported by NSF grants from the probability program. Levin was supported by the Sloan Foundation Grant 97-3-5.

REFERENCES

CHESSON, P. L. (1981). Models for spatially distributed populations: the effect of within patch variability. *Theor. Popul. Biol.* **19,** 288–325.

CHESSON, P. L. (1985). Coexistence of competitors in spatially and temporally varying environments: a look at the combined effects of different sorts of variability. *Theor. Popul. Biol.* **28,** 263–287.

COMINS, H. N. & HASSELL, M. P. (1996). Persistence of multispecies host-parasitoid interactions in spatially distributed models with local dispersal. *J. theor. Biol.* **183,** 19–28.

DEMASI, A., FERRARI, P. & LEBOWITZ, J. (1986). Reaction diffusion equations for interacting particle systems. *J. Stat. Phys.* **44,** 589–644.

DEROOS, A. M., MCCAULEY, E. & WILSON, W. G. (1991). Mobility versus density-limited predator-prey dynamics on different spatial scales. *Proc. Roy. Soc. Lond.* **246,** 117–122.

DURRETT, R. (1993). Predator-prey systems. In: *Asymptotic Problems in Probability Theory*: *Stochastic Models and Diffusions on Fractals* (Elworthy, K. D. & Ikeda, N., eds), pp. 37–58. Pitman Research Notes, Vol. 83. Essex, England: Longman Scientific.

DURRETT, R. (1995). Ten lectures on particle systems. *Ecole d'Eté de Probabilités de Saint Flour*, 1993. Lecture Notes in Math, Vol. 1608. Berlin: Springer.

DURRETT, R. (1999). Stochastic spatial models. *SIAM Rev.* **41,** 677–718.

DURRETT, R. & LEVIN, S. (1994). The importance of being discrete (and spatial). *Theor. Popul. Biol.* **46,** 363–394.

DURRETT, R. & NEUHAUSER, C. (1994). Particle systems and reaction diffusion equations. *Ann. Probab.* **22,** 289–333.

FLIERL, G., GRÜNBAUM, D., LEVIN, S. A. & OLSON, D. (1999). Individual-based perspectives on grouping. *J. theor. Biol.* **196,** 397–454.

HANSKI, I. (1998). Metapopulation dynamics. *Nature* **396,** 41–49.

HANSKI, I. A. & GILPIN, M. E. (1996). *Metapopulation Biology*: *Ecology*, *Genetics*, *and Evolution*. New York: Academic Press.

HARRIS, T. E. (1977). A correlation inequality for Markov processes in partially ordered spaces. *Ann. Probab.* **5,** 451–454.

HASSELL, M. P., COMINS, H. N. & MAY, R. M. (1991). Spatial structure and chaos in insect population dynamics. *Nature* **353,** 255–258.

HILBORN, R. (1975). The effect of spatial heterogeneity on the persistence of predator–prey interactions. *Theor. Popul. Biol.* **8,** 346–355.

HUFFAKER, C. B. (1958). Experimental studies on predation: dispersion factors and predator–prey oscillations. *Hilgardia* **27,** 343–383.

KEELING, M. J., MEZIC, I., HENDRY, R. J., MCGLADE, J. & RAND, D. A. (1997). Characteristic length scales of spatial models in ecology. *Philos. Trans. Roy. Soc. Lond. B* **352** (1361), 1589–1601.

KOPELL, N. & HOWARD, L. N. (1973). Plane wave solutions to reaction diffusion equations. *Stud. Appl. Math.* **42,** 291–328.

KOPELL, N. & HOWARD, L. N. (1974). Pattern formation in the Belousov reaction. *Lectures on Math in the Life Science.* **7,** American Math Society.

KOPELL, N. & HOWARD, L. N. (1981). Target patterns and spiral solutions to reaction diffusion equations with more than one space dimension. *Adv. Appl. Math.* **2,** 417–449.

LEVIN, S. A. (1974). Dispersion and population interactions. *Am. Nat.* **108,** 207–208.

LEVIN, S. A. (1992). The problem of pattern and scale in ecology. *Ecology* **73,** 1943–1967.

LEVIN, S. A. & SEGEL, L. A. (1976). Hypothesis on the origin of planktonic patchiness. *Nature* **259,** 5545.

LEVIN, S. A. & SEGEL, L. A. (1985). Pattern generation in space and aspect. *SIAM Rev.* **27,** 45–67.

MAY, R. M. (1994). Spatial chaos and its role in ecology and evolution. In: *Frontiers in Mathematical Biology*, pp. 326–344. Lecture Notes in Biomathematics, Vol. 100. New York: Springer.

MAY, R. M. (1995). Necessity and chance: deterministic chaos in ecology and evolution. *Bull. AMS*, *New Series.* **32,** 291–308.

MAYNARD SMITH, J. (1974). *Models in Ecology*. Cambridge: Cambridge University Press.

MCCAULEY, E., WILSON, W. G. & DEROOS, A. M. (1993). Dynamics of age-structured, and spatially structured predator–prey interactions: individual based models and population level formulations. *Am. Nat.* **142,** 412–442.

MIMURA, M. (1979). Asymptotic behaviors of a parabolic system related to a planktonic prey and predator model. *SIAM J. Appl. Math.* **37,** 499–512.

MIMURA, M., NISHIURA, Y. & YAMAGUCHI, M. (1979). Some diffusive prey and predator equations and their bifurcation problems. *Bifurcation Theory and Applications in Scientific Disciplines* (Guret, O. & Roseler, O. E., eds), Ann of NY Academy of Sciences, Vol. 310.

MURRAY, J. D. (1989). *Mathematical Biology*. Berlin: Springer.

MURRAY, J. D. (1990). Discussion: Turing's theory of morphogenesis — Its influence on modelling biological pattern and form. *Bull. Math. Biol.* **52,** 119–152.

NACHMAN, G. (1987a). Systems analysis of acarine predator prey interactions, I. A stochastic simulation model of spatial processes. *J. Animal Ecol.* **56,** 247–265.

NACHMAN, G. (1987b). Systems analysis of acarine predator prey interactions, II. The role of spatial processes in system stability. *J. Animal Ecol.* **56,** 267–281.

NEUBERT, M. G., KOT, M. & LEWIS, M. A. (1995). Dispersal and pattern formation in a discrete-time predator–prey model. *Theor. Popul. Biol.* **48,** 7–43.

NOWAK, M. A. & MAY, R. M. (1992). Evolutionary games and spatial chaos. *Nature* **359,** 826–829.

NOWAK, M. A. & MAY, R. M. (1993). The spatial dilemmas of evolution. *Int. J. Bifur. Chaos* **3,** 35–78.

NOWAK, M. A., BONHOEFFER, S. & MAY, R. M. (1994). More spatial games. *Int. J. Bifur. Chaos* **4,** 33–56.

PASCUAL, M. & CASWELL, H. (1997). Environmental heterogeneity and biological pattern in a chaotic predator–prey system. *J. theor. Biol.* **185,** 1–13.
PASCUAL, M. & LEVIN, S. A. (1999). From individuals to population densities: searching for the intermediate scale of nontrivial determinism. *Ecology* **80,** 207–228.
PIMENTEL, D., NAGLE, W. P. & MADDEN, J. L. (1963). Space-time structure of the environment and the survival of parasite-host systems. *Am. Nat.* **98,** 141–167.
RAND, D. A., KEELING, M. & WILSON, H. B. (1995). Invasion stability and evolution to criticality in spatially extended, artificial host–pathogen ecologies. *Proc. Roy. Soc. Lond. B* **259,** 55–63.
RAND, D. A. & WILSON, H. B. (1995). Using spatio-temporal chaos and intermediate scale determinism in artificial ecologies to quantify spatially-extended systems. *Proc. Roy. Soc. Lond.* **259,** 111–117.
SATULOVSKY, J. (1996). Lattice Lotka–Volterra models and negative cross-diffusion. *J. theor. Biol.* **183,** 381–389.
SATULOVSKY, J. & TOME, T. (1994). Stochastic lattice gas model for a predator–prey system. *Phys. Rev. E.* **49,** 5073–5079.
SEGEL, L. A. & JACKSON, J. L. (1972). Dissipative structure: an explanation and an ecological example. *J. theor. Biol.* **37,** 545–559.
SEGEL, L. A. & LEVIN, S. A. (1976). Application of nonlinear stability theory to the study of the effects of dispersion on predator prey interactions. *Selected Topics in Statistical Mechanics and Biophysics* (Piccirelli, R. A., ed.), AIP Conference Proceedings, Vol. 27.
TURING, A. M. (1952). The chemical basis of morphogenesis. *Philos. Trans. Roy. Soc. B* **327,** 37–72.
WILSON, W. G. (1996). Lotka's game in predator–prey theory: linking populations to individuals. *Theor. Popul. Biol.* **50,** 368–393.
WILSON, W. G., DEROOS, A. M. & MCCAULEY, E. (1993). Spatial instabilities within the diffusive Lotka–Volterra system: individual-based simulation results. *Theor. Popul. Biol.* **43,** 91–127.
WINFREE, A. T. (1987). *When Time Breaks Down.* Princeton, NJ: Princeton University Press.

APPENDIX A

Analysis of the ODE and the PDE

Here, we analyse the linearized equation

$$\begin{aligned} dv_1/dt &= Fv_1 + Gv_2, \\ dv_2/dt &= Hv_1, \end{aligned} \tag{A.1}$$

where $F = A'(\bar{u}_1) - \bar{u}_2 B'(\bar{u}_1)$, $G = -B(\bar{u}_1)$, and $H = u_2 C'(\bar{u}_1)$. Letting M be the matrix with first row (F, G) and second row $(H, 0)$ we have

$$\begin{aligned} \text{trace}(M) &= F = A'(\bar{u}_1) - \bar{u}_2 B'(\bar{u}_1), \\ \det(M) &= -GH > 0. \end{aligned} \tag{A.2}$$

The determinant being positive implies that the two eigenvalues λ_1 and λ_2 are either (i) both real and of the same sign or (ii) a complex conjugate pair. In either case, when the trace is positive, both $\text{Re}(\lambda_i)$ must be positive, and when the trace is negative both $\text{Re}(\lambda_i)$ must be negative. It follows from this that if the trace changes sign at a point where the determinant is positive, then two eigenvalues are a purely imaginary conjugate pair.

The last paragraph describes the *Hopf bifurcation* mentioned in the theorem. To investigate the trace to see when the sign change occurs, we use the equilibrium equation $\bar{u}_2 = A(\bar{u}_1)/B(\bar{u}_1)$ and write

$$\begin{aligned} F &= A'(\bar{u}_1) - \frac{A(\bar{u}_1)}{B(\bar{u}_1)} B'(\bar{u}_1) \\ &= \frac{A'B - AB'}{B} = B\left(\frac{A}{B}\right)', \end{aligned} \tag{A.3}$$

where in the last two expressions we have omitted the argument $\bar{u}_1$ since it is always the same. Our next step is:

Lemma A.1. *B/A is convex on* $[0, 1]$.

Proof. The ratio

$$\frac{B(x)}{A(x)} = \frac{1}{1-x} + \frac{S_q(x)}{\beta_1} \quad \text{where}$$

$$S_q(x) = \frac{1 - (1-x)^q}{x(1-x)}. \tag{A.4}$$

The function $1/(1-x)$ is convex on $[0, 1]$, so to complete the proof we can verify by induction that $S_q(x)$ also has this property. When $q = 1$, $S_1(x) = 1/(1-x)$ and the result is true. If $q \geqslant 2$ the difference

$$\begin{aligned} S_q(x) - S_{q-1}(x) &= \frac{(1-x)^{q-1} - (1-x)^q}{x(1-x)} \\ &= (1-x)^{q-2} \end{aligned}$$

is convex on (0,1). Since $S_{q-1}(x)$ is convex by the induction hypothesis, the desired conclusion follows. □

Lemma A.1 implies that if $B(x)/A(x)$ is increasing for small x then it is increasing for all $x > 0$. Taking reciprocals we have proved.

Lemma A.2. *If the derivative of B/A is positive at 0 then A/B is decreasing for all $x > 0$.*

With eqn (A.3), this implies that the trace is always negative, i.e. the fixed point is locally attracting. Our final task then is to evaluate the derivative of B/A at $x = 0$. Expanding $(1 - x)^q$ using binomial coefficients, we see that

$$(1 - x)S_q(x) = \frac{1 - (1 - x)^q}{x} = \sum_{j=1}^{q} \binom{q}{j}(-x)^{j-1}.$$

Writing $R(x) = B(x)/A(x)$ and using eqn (A.4), it follows that

$$R(x) = (1 - x)^{-1}\{1 + (1 - x)S_q(x)/\beta_1\}$$

$$= (1-x)^{-1}\left\{1+\frac{1}{\beta_1}\sum_{j=1}^{q}\binom{q}{j}(-x)^{j-1}\right\}. \quad \text{(A.5)}$$

Differentiating and then setting $x = 0$ we find

$$R'(0) = \left(1+\frac{q}{\beta_1}\right)-\frac{q(q-1)}{2\beta_1} = 1-\frac{q(q-3)}{2\beta_1}. \quad \text{(A.6)}$$

If $0 \leqslant q \leqslant 3$ then $R'(0)$ is always positive. For $q > 3$, $R'(0)$ will be negative for small values of β_1.

The instability of the interior fixed point implies that orbits that start near it will begin to spiral outwards. To complete the proof of the existence of a periodic orbit we have to stop this trajectory from reaching the fixed point $(u_1, u_2) = (0, 0)$. To do this, and to prepare for the study of the PDE, we construct a function h that will be a *Lyapunov function* near the *extinction boundaries*, $u_1 = 0$ and $u_2 = 0$.

Lemma A.3. If the positive constants a, b, c, f and ε are chosen appropriately then

$$g(t) = h(u_1(t), u_2(t)) = -a\log u_1(t) - b\log u_2(t) + cu_1(t) + fu_2(t) \quad \text{(A.7)}$$

is decreasing when $u(t) \in \Gamma_\varepsilon = \{u : 0 \leqslant \min\{u_1, u_2\} \leqslant \varepsilon, u_1 + u_2 \leqslant 1\}$.

Proof. We begin by choosing the first four constants. We make our choices now to demonstrate that is possible to simultaneously satisfy all our desires. Let $b = 1$ and $c = 1$. Pick a large enough so that

(i) $$-a\beta_1 + b\delta < 0,$$

(ii) $$c < a/2,$$

(iii) $$-(a\beta_1/2)(1 - \bar{u}_1) + b\delta < 0.$$

Then pick f large enough so that (iv) $a(\beta_1 + q + 1) - f\delta/2 < 0$. The reader will see the reason for our interest in inequalities (i)–(iv) later.

Differentiating and recalling the mean-field ODE given in eqns (1) and (2) we see that

$$\frac{dg}{dt} = \left(-\frac{a}{u_1} + c\right)\frac{du_1}{dt} + \left(-\frac{b}{u_2} + f\right)\frac{du_2}{dt}$$

$$= (cu_1 - a)\left\{\beta_1(1-u_1-u_2) - u_2\left(\frac{1-(1-u_1)^q}{u_1}\right)\right\}$$

$$+ (fu_2 - b)\{\beta_2 - (\beta_2 + \delta)(1-u_1)^q\}. \quad \text{(A.8)}$$

$1-(1-u_1)^q \sim qu_1$ as $u_1 \to 0$, so when $u_1 = 0$ the r.h.s. becomes

$$-a\{\beta_1 - (\beta_1 + q)u_2\} + (fu_2 - b)(-\delta)$$

$$= (-a\beta_1 + b\delta) + \{a(\beta_1 + q) - f\delta\}u_2. \quad \text{(A.9)}$$

Conditions (i) and (iv) make this negative and bounded away from 0 for $0 \leqslant u_2 \leqslant 1$. It then follows from continuity that there is an $\varepsilon_1 > 0$ so that the expression in eqn (A.8) is negative when $0 \leqslant u_1 \leqslant \varepsilon_1$ and $0 \leqslant u_2 \leqslant 1 - u_1$.

At the other boundary, which contains the fixed point (1, 0), we have to argue more carefully. Keeping in mind that u_2 will be small, but not using this in the computation, we can rearrange the r.h.s. of eqn (A.8) to get

$$(cu_1 - a)\beta_1(1 - u_1) - b\{\beta_2 - (\beta_2 + \delta)(1 - u_1)^q\} + u_2\left((a - cu_1)\left\{\beta_1 + \frac{1 - (1 - u_1)^q}{u_1}\right\} + f\{\beta_2 - (\beta_2 + \delta)(1 - u_1)^q\}\right). \tag{A.10}$$

When $u_2 = 0$, the second line vanishes. Choice (ii) guarantees the first term on the first line is negative. Recall $u_1 \leqslant 1$. The second term on the first line, $\beta_2 - (\beta_2 + \delta)(1 - u_1)^q \geqslant 0$ for $u \geqslant \bar{u}_1$. For $u \leqslant \bar{u}_1$, note that choices (ii) and (iii) imply

$$(cu_1 - a)\beta_1(1 - u_1) - b\{\beta_2 - (\beta_2 + \delta)(1 - u_1)^q\} \leqslant (-a\beta_1/2)(1 - \bar{u}_1) + b\delta < 0.$$

At this point, our choices have guaranteed that the expression in eqn (A.10) is non-positive on the boundary $\bar{u}_2 = 0$. Since eqn (A.10) tends to 0 as the fixed point (1, 0) is approached we have to look separately at the points in the triangle Γ near $u_1 = 1$. Let $\eta > 0$ be chosen so that if $u_1 \geqslant 1 - \eta$ then

(v) $$u_1 > \bar{u}_1,$$

(vi) $$\frac{1 - (1 - u_1)^q}{u_1} \leqslant 1 + q,$$

(vii) $$\beta_2 - (\beta_2 + \delta)(1 - u_1)^q < -\delta/2.$$

(v) implies that the second term on the first line in eqn (A.10) is $\leqslant 0$, so using choices (ii), (vi), and (vii) the expression in eqn (A.10) is at most

$$-\frac{a\beta_1}{2}(1 - u_1) + u_2\left(a(\beta_1 + q + 1) - \frac{f\delta}{2}\right) < 0$$

the final < 0 due to choice (iv).

This completes our analysis of the third term of eqn (A.10), so we can now assert that there is an $\varepsilon_2 > 0$ so that the expression in eqn (A.10) is negative when $0 \leqslant u_2 \leqslant \varepsilon_2$ and $0 \leqslant u_1 \leqslant 1 - u_2$. Taking ε to be the minimum of ε_1 and ε_2 completes the proof of Lemma A.3. □

With the proof of Lemma A.3 completed the hard work is done. Our next step is to modify h to be a Lyapunov function on all of $\Gamma = \{(u_1, u_2): u_i \geqslant 0, u_1 + u_2 \leqslant 1\}$ by making it constant, a short distance from the boundaries of interest. To pick a truncation level we note that h is continuous on Γ and finite except if u_1 or u_2 is 0, so we can pick M large enough so that $\{u \in \Gamma : h(u) \geqslant M\} \subset \Gamma_\varepsilon$. To make a differentiable truncation of h, we introduce

$$\psi(x) = \begin{cases} M & \text{if } x \leqslant M \\ M + (x - M)^2 & \text{if } x \geqslant M \end{cases}$$

and set $\bar{h}(x) = \psi(h(x))$.

Lemma A.4. *$\bar{h}$ is a convex Lyapunov function.*

Proof. The Lyapunov property follows from Lemma A.3, the choice of M made above, and the fact that ψ is non-decreasing. To check convexity, we observe that h is convex, being the sum of four convex functions, and ψ is non-decreasing and convex. It follows from this that if $z, w \in \Gamma$ and $\lambda \in [0, 1]$ then

$$\psi(h(\lambda z + (1 - \lambda)w)) \leqslant \psi(\lambda h(z) + (1 - \lambda)h(w)) \leqslant \lambda\psi(h(z)) + (1 - \lambda)\psi(h(w)).$$

This demonstrates the convexity of $\bar{h}$ and completes the proof of Lemma A.4. □

Proof of Theorem 2. With Lemma A.4 established, the desired result now follows from calculations in Section 2 of Durrett (1993). □